

# Flocculation of Kaolinite Clay Suspensions Using a Temperature-Sensitive Polymer

Hongjun Li, Jun Long, Zhenghe Xu, and Jacob H. Masliyah

Dept. of Chemical and Materials Engineering, University of Alberta, Edmonton, Alberta T6G 2G6, Canada

DOI 10.1002/aic.11073

Published online December 18, 2006 in Wiley InterScience (www.interscience.wiley.com).

*A temperature-sensitive polymer, poly(N-isopropylacrylamide) [poly(NIPAM)], was tested to flocculate kaolinite clay suspensions. Settling tests at both room temperature and 40°C were carried out. The results show that settling at 40°C resulted in significantly higher settling rates and smaller sediment volumes. This behavior indicates that the polymer molecules changed from a stretched structure to a coil-like conformation with increasing temperature. It is the change in conformation that induced more compacted flocs, thus resulting in faster settling. To understand the role of temperature in the flocculation, the long-range interaction and adhesion forces between kaolinite clay particles in the polymer solutions at both room temperature and 40°C were measured using an atomic force microscope (AFM). The measured adhesion forces correlated well with the settling characteristics: a stronger adhesion led to a higher initial settling rate. The retraction force profiles obtained at different temperatures confirmed the conformational change of the polymer with temperature. © 2006 American Institute of Chemical Engineers AIChE J, 53: 479–488, 2007*

**Keywords:** poly(N-isopropylacrylamide), thermosensitive polymer, flocculation, colloidal force, AFM

## Introduction

Flocculation of fine clays has a wide range of practical implications. In water-based processes used to extract bitumen from oil sands, for example, the produced tailing slurry is discharged into tailings ponds for solid–liquid separation. Because of the very slow settling of fine solids in the tailing ponds, there is a large accumulation of fine tailings inventory with trapped water. It was estimated that the volume of the mature fine tailings (MFT), the aged aqueous suspension of fines, will increase to over one billion cubic meters by the year 2020.<sup>1</sup> Flocculating fine solids in the produced tailings would facilitate tailings management.

Over the last several years, many attempts have been made to reduce the tailing volume by various treatments.<sup>2–5</sup> Several processes were developed, including the composite tailings

(CT) process<sup>2</sup> and paste technology.<sup>4,5</sup> In the CT process, gypsum and coarse sands are added to the MFT to cause nonsegregating sediments with quick release of water for recycle. However, gypsum addition can lead to an elevated concentration of calcium in the recycled process water. A high concentration of calcium in the process water has been found to be detrimental to bitumen recovery.<sup>4</sup> In paste technology polymers are added to flocculate the fine clays, thickening them into a paste. Cymerman et al.<sup>4</sup> found anionic polyacrylamides with high molecular weight and medium charge density were effective in flocculating the oil sand fines in tailings. However, the formed flocs are usually loosely packed and trap a large amount of water, which is very difficult to release.<sup>6</sup> Consequently, it is desirable to design flocculants that achieve more compacted flocs to achieve faster release of water.

Temperature-sensitive polymer flocculants were recently found to be able to form much denser flocs than polyacrylamides.<sup>6</sup> Temperature-sensitive polymers exhibit a phase transition with temperature. Usually, temperature-sensitive polymers are hydrophilic and soluble in water when the tempera-

Correspondence concerning this article should be addressed to J. H. Masliyah at Jacob.Masliyah@ualberta.ca.

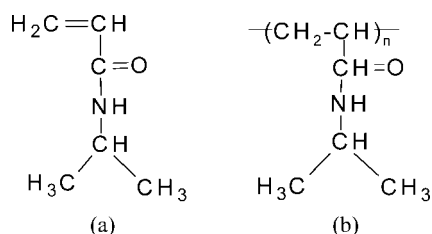


**Figure 1. (a) Molecular structure of the monomer of *N*-isopropylacrylamide; (b) molecular structure of poly(*N*IPAM).**

ture is below their phase-transition temperature (PTT), but they become hydrophobic and insoluble when the solution temperature is above their PTT.<sup>7,8</sup> The hydrophilic/hydrophobic transition is reversible. A representative nonionic temperature-sensitive polymer is poly(*N*-isopropylacrylamide) [poly(*N*IPAM)], which has a transition temperature of about 32°C.<sup>9</sup>

Guilet et al.<sup>10</sup> described flocculation of suspended particles using temperature-sensitive polymers. The main claim of their patent was that below the transition temperature, temperature-sensitive polymers were effective flocculants, exhibiting a behavior similar to that of polyacrylamides, whereas above the transition temperature, they became poor flocculants. In contrast, others<sup>11–14</sup> found that temperature-sensitive polymers could induce a flocculation even at a temperature above the transition temperature. This discrepancy may be attributable to the different procedures used in the mixing and flocculation steps.

Because flocculation is controlled by interactions between suspended particles and polymers, often causing a drastic change in interactions between the particles, direct measurement of the interaction forces between the particles in polymer solutions would provide a quantitative study of flocculation behaviors. In recent years, atomic force microscopy (AFM) has been widely used for direct colloidal force measurements.<sup>15–19</sup> To provide fundamental insights into the role of a temperature-sensitive polymer as a flocculant in fine clay flocculation, in the current study, colloidal forces between clay particles in aqueous solutions were directly measured using AFM. The measured forces were correlated with the settling results of clay suspensions.

## Experimental

### Polymer preparation

Poly(*N*-isopropylacrylamide) [poly(*N*IPAM)], a representative of temperature-sensitive polymers, was synthesized by free-radical polymerization, following procedures described by Guillet and Heskins.<sup>10</sup> The monomer *N*-isopropylacrylamide was obtained from Fisher Scientific (Pittsburgh, PA). The molecular structures of *N*-isopropylacrylamide and poly(*N*IPAM) are shown in Figures 1a and 1b, respectively. The initiator and accelerator used in the polymerization were potassium persulfate (99.99%) and potassium bisulfate (>99%), respectively (both from Sigma-Aldrich, St. Louis, MO). A list of chemicals used in the synthesis of poly(*N*IPAM) is given in Table 1. More specifically, a 100 g/L *N*-isopropylacrylamide solution was prepared using deionized water, and 200 mL of the pre-

pared solution was fed into a 250-mL reactor with a stirrer, a gas inlet, and outlet. The reactor was degassed by successively purging with high-purity nitrogen for 1 h. In the course of being stirred, 4 mL of 5.0 g/L potassium bisulfate was added to the solution followed by the addition of 8 mL of 5.0 g/L potassium persulfate. The polymerization proceeded at room temperature for 2 days. After the polymerization, the mixture was first diluted with 500 mL deionized water. The diluted solution was left undisturbed for 2 days, after which it was heated to 50°C, at which temperature the polymer became insoluble and precipitated. The precipitated polymer was separated from the solution by filtration. The polymer retained as a filter cake was purified again by redissolving it in deionized water at room temperature, heating to 50°C, and then filtrating following the same procedure described above. This purification process was repeated three times. The final collected filter cake was placed in a vacuum oven at 60°C and 0.3 kPa for 1 day to evaporate the entrapped water. The final polymer product was then obtained.

### Settling tests

**Clay Suspension Preparation.** Clay suspensions were prepared by dispersing kaolinite clays (Wards Natural Science Ltd., Ontario, Canada) in deionized water to 10 wt % of solids. The pH of the suspensions was adjusted to 8.6. A 5 g/L poly(*N*IPAM) stock solution was prepared by dissolving the prepared polymer in deionized water at room temperature. Settling tests were conducted in 100-mL graduated cylinders. In this study, the following two settling procedures were used.

- Procedure A—Settling at room temperature

A 100-mL clay suspension was transferred into a 250-mL beaker. A magnetic stirrer was used to mix the suspension at 1000 rpm for 2 min. While the suspension was being stirred, a predetermined volume of polymer solution was added. After the mixing, the suspension was carefully transferred into a 100-mL graduated cylinder. After inverting the cylinder a few times, the cylinder was allowed to stand still, during which the interface mud line<sup>20</sup> (that is, the interface between the supernatant liquid at the top and the concentrated suspension layer at the bottom) as a function of time was recorded. In this procedure, the temperature was maintained at room temperature throughout the whole process.

- Procedure B—Settling at 40°C

In procedure B, the mixing of the polymer with a kaolinite suspension was performed at room temperature, following the same procedure described above. The suspension was then heated to 40°C using a heater while still being stirred. A thermometer was used to control the suspension temperature. When the temperature reached 40°C, the stirring was stopped and the suspension was transferred to a 100-mL graduated cylinder. A thermostatic water bath was used to keep the suspension temperature at 40°C. The cylinder was inverted a few times and left still in the water bath. The mud line as a function

**Table 1. Chemicals Used in the Synthesis of Poly(*N*IPAM)**

		Concentration
Monomer	<i>N</i> -Isopropylacrylamide	0.1 g/mL
Initiator	Potassium persulfate	200 ppm
Accelerator	Potassium bisulfate	100 ppm

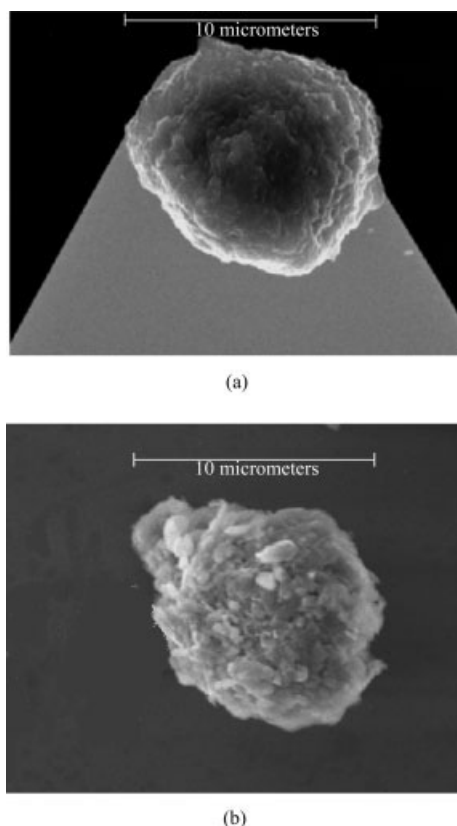


**Figure 2. (a) A kaolinite clay probe; (b) a kaolinite clay particle glued on a substrate.**

of time was then recorded. The sediment volume (that is, the volume of the concentrated suspension layer) was plotted as a function of time—referred to as the *settling curve*—which allows us to determine the initial settling rate (m/h) from the slope of the initial linear portion of the curve.<sup>4,21</sup>

**Clay Probe Preparation.** Kaolinite particles with a pseudospherical shape were selected as the probe for the colloidal force measurements. The particles were chosen from a larger number of kaolinite particles under an optical microscope. The chosen kaolinite particle was glued onto the tip of an AFM cantilever (lever-type, 100  $\mu\text{m}$  wide) with a spring constant of 0.58 N/m using a two-component epoxy (EP2LV, Master Bond, Hackensack, NJ). The glued clay probes, such as the one shown in Figure 2a, were allowed to set in a vacuum desiccator for >24 h. Before the force measurements, the prepared probes were thoroughly rinsed with deionized water and ethanol followed by blow-drying with ultrapure-grade nitrogen. The probes were then exposed to an ultraviolet light (115 V, 60 Hz, 0.48 A, Model SP-1, UVP, Inc., Upland, CA) for >5 h to remove any possible organic contaminants. The exact size of the kaolinite clay particle used was determined with an optical microscope before the force measurements. More details on colloid probe preparation are provided elsewhere.<sup>22,23</sup>

**Substrate Preparation.** Kaolinite particles were glued onto silica wafers of 12  $\times$  12 mm<sup>2</sup>. As in probe preparation, only a very small amount of the two-component epoxy was used under an optical microscope. To dry the glue, the prepared substrates were placed in a vacuum desiccator for 1 day. Before

force measurements, the prepared substrates were thoroughly rinsed with deionized water and ethanol, followed by blow-drying with the ultrapure-grade nitrogen. The substrates were then exposed to an ultraviolet light for >5 h to remove any possible organic contaminants. Figure 2b shows glued kaolinite particles on a substrate.

### Surface force measurement

Surface force measurement was conducted using a Nanoscope E AFM (Digital Instruments, Santa Barbara, CA) with a vender-supplied fluid cell. A prepared substrate was mounted on the piezoelectric transition stage. A clay probe was mounted in the fluid cell. To position a kaolinite probe just over a kaolinite particle glued onto the substrate surface, an optical viewing and positioning system (Digital Instruments) was used. In our experiment, a prepared solution was slowly injected into the fluid cell with great care to avoid the trapping of air bubbles. The system was allowed to incubate for 1 h at room temperature before the first approach of the probe to the substrate. In the force measurements, the piezoelectric transition stage brought the substrate with kaolinite particles to approach or retract from the probe particle in the vertical ( $z$ ) direction. The forces between the probe and a particle on the substrate surface were determined from the deflection of the cantilever using Hooke's law. Each force plot represents a complete extension/retraction cycle of the piezo. When the substrate approached the probe, the long-range interaction between the two particles was measured, whereas the adhesion (or pull-off) force between them was obtained during the retraction process after contact was made. For the force measurements conducted at 40°C, a heater and a thermometer (Digital Instruments) were used to control the temperature in the fluid cell. Because the kaolinite clay particles were irregular, to obtain representative results, each experiment was performed with three kaolinite-kaolinite probe pairs and repeated twice for each pair. For each test condition, hundreds of force profiles were recorded. For quantitative comparison, the measured long-ranged interaction force ( $F$ ) and adhesion force were normalized by the probe radius ( $R$ ). A more detailed description on the colloidal force measurement using AFM can be found elsewhere.<sup>24–26</sup>

## Results and Discussion

### Molecular weight of poly(NIPAM)

The molecular weight of poly(NIPAM) was estimated by measuring the viscosity of a series of the polymer-in-tetrahydrofuran solutions at 27°C using a Ubbelohde viscometer (Fisher Scientific). The viscosity of a polymer solution varies with polymer concentration according to the following equation:<sup>27</sup>

$$[\eta] = \lim_{c \rightarrow 0} [(\eta - \eta_0)/\eta_0 c] = \lim_{c \rightarrow 0} (\eta_{sp}/c)$$

where  $\eta$  is the viscosity of a polymer solution of concentration  $c$ ,  $\eta_0$  is the viscosity of pure solvent,  $[\eta]$  is the intrinsic viscosity,  $\eta_{sp}$  is the specific viscosity, and  $c$  is the concentration of polymer solution in g/L. The value of  $[\eta]$  can be experimentally determined from the y-intercept by plotting the reduced viscosity ( $\eta_{sp}/c$ ) as a function of the polymer concentration.

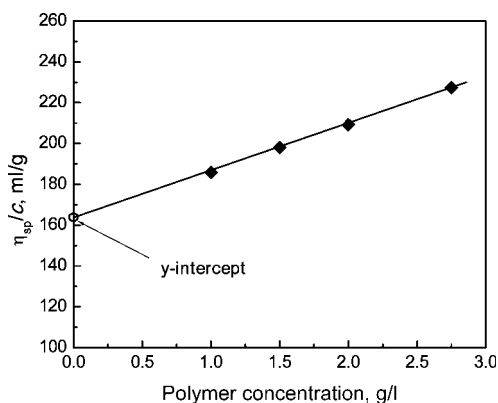


**Figure 3.** Relationship between  $\eta_{sp}/c$  and the polymer concentration in tetrahydrofuran.

Figure 3 shows the results of the reduced viscosity as a function of the polymer concentration in tetrahydrofuran. A good linear relationship was obtained. From the y-intercept, as indicated by the arrow in the figure, the value of  $[\eta]$  was determined to be 162 mL/g. The number-average molecular weight  $\bar{M}_n$  is related to intrinsic viscosity of polymer by

$$[\eta] = 9.59 \times 10^{-3} \bar{M}_n^{0.65}$$

From this equation, details of the method to measure the molecular weight of poly(NIPAM) can be found elsewhere.<sup>12,28</sup> The number-average molecular weight of the polymer was cal-

culated to be  $3.2 \times 10^6$ . Polymers with such an average molecular weight are suitable as flocculants.

### Settling tests

**Results of Procedure A.** Figure 4 shows the effect of poly (NIPAM) on the settling of 10 wt % kaolinite suspensions at room temperature. With increasing polymer addition from 0 to 50 ppm, the initial settling rate increased from 0.01 to 0.05 m/h (Figure 4a). Above this dosage level, the initial settling rate decreased with further increasing the polymer dosage. When the polymer dosage was at 200 ppm, the initial settling rate became nearly zero. In this case, the kaolinite suspension actually became well dispersed by the added polymers. Figure 4b shows that when the polymer dosage increased from 0 to 50 ppm, the sediment volume after a settling period of 120 min decreased from 92 to 75 mL. A further increase in the polymer dosage caused an increase in sediment volume. It is speculated that at the optimal polymer dosage (that is, 50 ppm), the surface of kaolinite clay particles was partially covered by the adsorbed polymers, which allows bridging between the kaolinite clay particles to form. At the dosage of 200 ppm, the surface of the kaolinite particles was fully covered by the adsorbed polymers. In this case, the adsorbed polymer layer sets a steric barrier to prevent the kaolinite particles from approaching each other; as a result, the suspension became more stabilized. These settling results were consistent with those reported in other studies.<sup>29,30</sup>

**Results of Procedure B.** Figure 5 shows the settling results of 10 wt % kaolinite suspensions obtained using procedure B

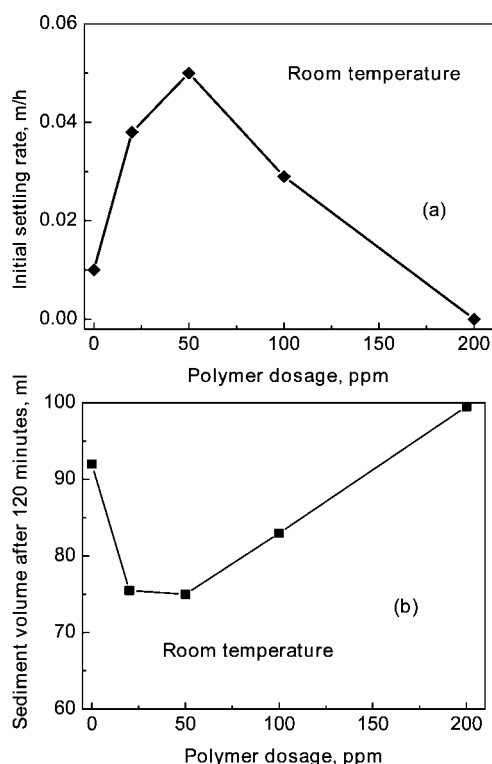


**Figure 4.** (a) Initial settling rate as a function of polymer dosage using procedure A; (b) sediment volume after a settling period of 120 min as a function of polymer dosage.

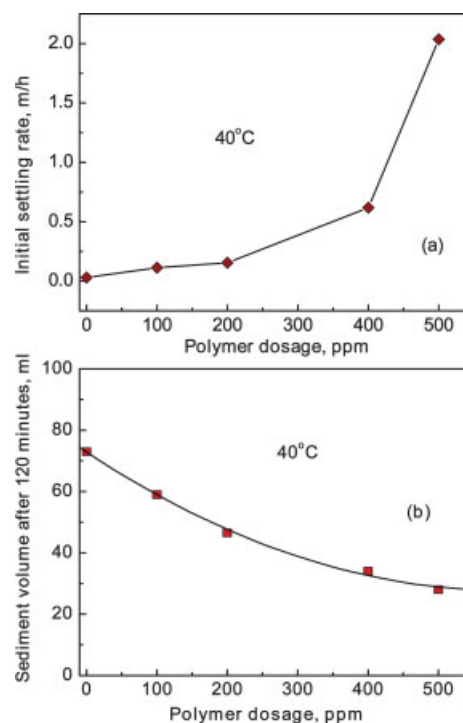


**Figure 5.** (a) Initial settling rate as a function of the polymer dosage using procedure B. (b) Sediment volume after a settling period of 120 min as a function of polymer dosage.

[Color figure can be viewed in the online issue, which is available at [www.interscience.wiley.com](http://www.interscience.wiley.com).]

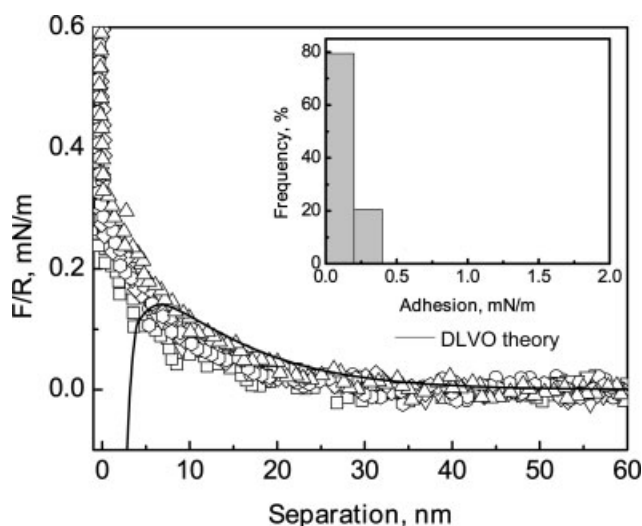


**Figure 6. Long-range interaction and adhesion forces between kaolinite particles in a 1 mM KCl solution at pH  $\approx$  8.6 at room temperature.**

The solid curve is the DLVO force profile using  $\psi = -35$  mV,  $\kappa^{-1} = 9.61$  nm and  $A = 2.20 \times 10^{-20}$  J. The inset shows the adhesion force distribution.

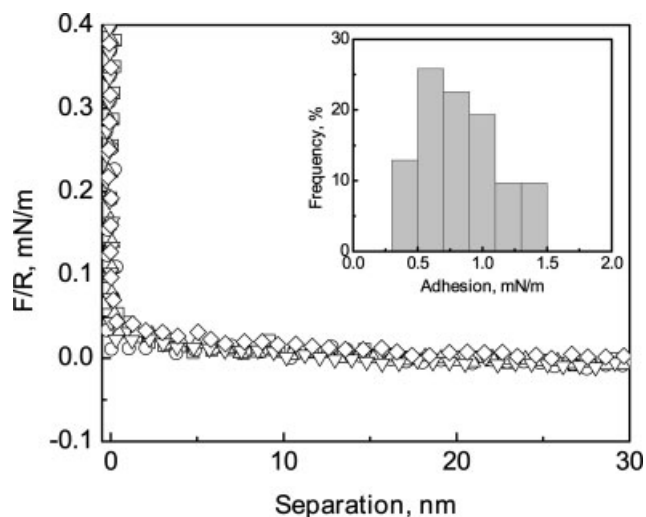
(that is, mixing at room temperature and then settling at 40°C). As shown in Figure 5a, the initial settling rate increased drastically when the polymer dosage was increased from 0 to 500 ppm. Accordingly, the sediment volume after a settling period of 120 min decreased considerably from 73 to 28 mL, as shown in Figure 5b. In a comparison of the settling results obtained using procedure B with those obtained using procedure A, it is clear that temperature has a significant impact on the settling. Using procedure A, the maximum initial settling rate was about 0.05 m/h obtained with 50 ppm polymer addition. In contrast, the initial settling rate of 2.0 m/h was obtained using procedure B in the presence of 500 ppm poly(NIPAM). Using procedure A, the smallest sediment volume after a settling period of 120 min was about 75 mL, whereas it was 28 mL in the presence of 500 ppm poly(NIPAM) using procedure B. These results indicate that the sediment formed using procedure B was more compacted than that using procedure A.

### AFM force measurements

**Results Obtained at Room Temperature.** To understand the role of poly(NIPAM) as a flocculant in the settling of kaolinite suspensions, the long-range interaction and adhesion forces between two kaolinite particles were measured by AFM. As a baseline, Figure 6 shows the measured forces in a 1 mM KCl solution at pH 8.6 without polymer addition. As anticipated, the data are fairly scattered as a result of the surface irregularity of the kaolinite particles. The long-range interaction force was purely repulsive. To find the dominant forces contributing to the long-range repulsion, the classical DLVO (Derjaguin–Landau–Verwey–Overbeek) theory was used to obtain theoretical force profiles.<sup>31</sup> The van der Waals force was calculated using Hamaker’s microscopic approach. The reported Hamaker constant ( $A$ ) of the mica–water–mica system,  $2.2 \times 10^{-20}$  J,<sup>31</sup> was used for the kaolinite–water–kaolinite system. The electrostatic double-layer force, on the other hand, was calculated

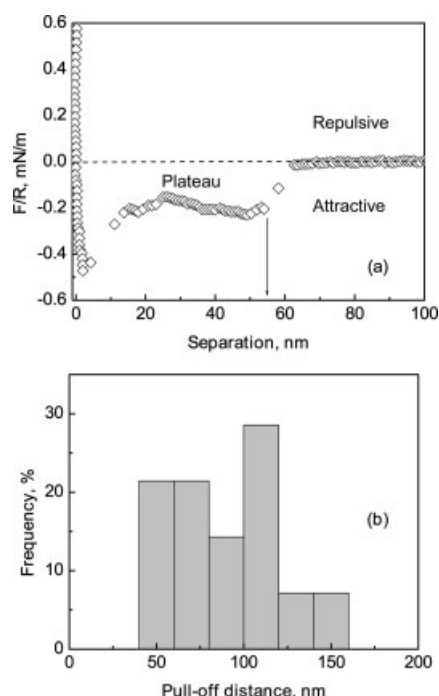
numerically by solving the nonlinear Poisson–Boltzmann equation, using a constant surface potential of the kaolinite surface as a boundary condition. The kaolinite clay surface is of constant surface potential because its surface charge arises primarily from adsorbed ions from solutions.<sup>32,33</sup> The measured zeta potential value (as an approximation of the Stern potential  $\psi_d$ ) of the kaolinite particles and the calculated decay length ( $\kappa^{-1}$ ) of the electrolytes medium were used to calculate the electric double-layer force. A zeta potential of kaolinite clay particles in a 1 mM KCl solution at pH 8.6 at room temperature was measured to be about  $-35$  mV using a Zetaphoremeter IV<sup>TM</sup> (SEPHY/CAD Instrumentations, Buckinghamshire, UK).<sup>34</sup> The decay length is 9.61 nm for the 1 mM KCl solution. A program developed by Liu et al.<sup>35</sup> was used to calculate the DLVO forces. As noted in Figure 6, the long-range force profiles at a separate distance  $>8$  nm substantially agree with the theoretical profile as shown by the solid curve in the figure. This indicates that the long-range forces were dominated by the electrostatic double-layer interactions. The adhesion force distribution is shown in the inset of Figure 6. In most cases, no adhesion was detected. Because the long-range force was repulsive and the adhesion was nearly zero, it would be anticipated that at room temperature the kaolinite suspension would be stable in a 1 mM KCl solution at pH 8.6 in the absence of the polymer. This expectation was verified in the settling tests. As discussed earlier under *Results of Procedure A*, the initial settling rate of kaolinite suspension in the absence of polymer at room temperature was small (0.01 m/h) and the sediment volume after a settling period of 120 min was 92 mL, which is very close to the volume of the original suspension of 100 mL.

Figure 7 shows the long-range interaction and adhesion forces between kaolinite clay particles in the presence of 20 ppm poly(NIPAM) at room temperature. With poly(NIPAM) addition, the long-range repulsive force decreased significantly, indicating that the electrostatic double-layer force was depressed by the polymer addition. Because the polymer is



**Figure 7. Long-range interaction and adhesion forces between kaolinite particles in a 1 mM KCl solution in the presence of 20 ppm poly(NIPAM) at pH  $\approx$  8.6 and room temperature.**

The inset shows the adhesion force distribution.



**Figure 8. (a) A typical retraction force profile obtained between kaolinite particles in a 1 mM KCl solution in the presence of 20 ppm poly(NIPAM) at pH  $\approx$  8.6 and room temperature; (b) a distribution of the pull-off distances obtained under the same conditions as in (a).**

nonionic, coverage of the surface by the polymer would screen out the surface charge of the kaolinite particles to reduce the electrostatic repulsive force. The flocculation of the kaolinite suspension at room temperature in the presence of poly(NIPAM) is attributed to the bridges between the kaolinite particles by the polymer. The bridging effect is verified by a typical retraction force profile at room temperature, as shown in Figure 8a. The two kaolinite surfaces, presumably connected by polymer chains, detached at a pull-off distance of about 60 nm. This observation suggests that poly(NIPAM) molecules at room temperature have a long, extended structure. A distribution of the pull-off distances is shown in Figure 8b. The pull-off distances obtained are in a range of 40 to 150 nm, indicating a polydispersity of the synthesized polymer. The adhesion force distribution as shown in the inset of Figure 7 is centered at 0.8 mN/m. Appearance of the adhesion force suggests the presence of forces holding the kaolinite particles together. The reduced repulsion and presence of adhesion would make it possible for the kaolinite particles to approach and then connect with each other, thereby resulting in flocculation between the particles. As mentioned in the settling results using procedure A, the suspension in the presence of 50 ppm polymer exhibited an initial settling rate of 0.05 m/h and a sediment volume of 75 mL after a settling period of 120 min, in contrast to a negligible settling without polymer addition, indicating a practical flocculation arising from the reduced repulsion and increased adhesion between the kaolinite particles by adequate polymer adsorption.

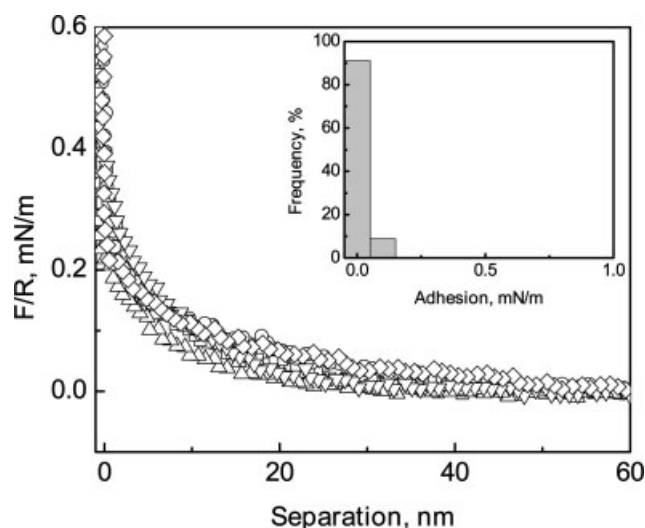


**Figure 9. Long-range interaction and adhesion forces between kaolinite particles in a 1 mM KCl solution in the presence of 50 ppm poly(NIPAM) at pH  $\approx$  8.6 and room temperature.**

The inset shows the adhesion force distribution.

Figure 9 shows the long-range repulsion and adhesion forces between kaolinite particles in a 1 mM KCl solution containing 50 ppm polymer at pH 8.6 and room temperature. The long-range repulsion became strong and the adhesion disappeared.

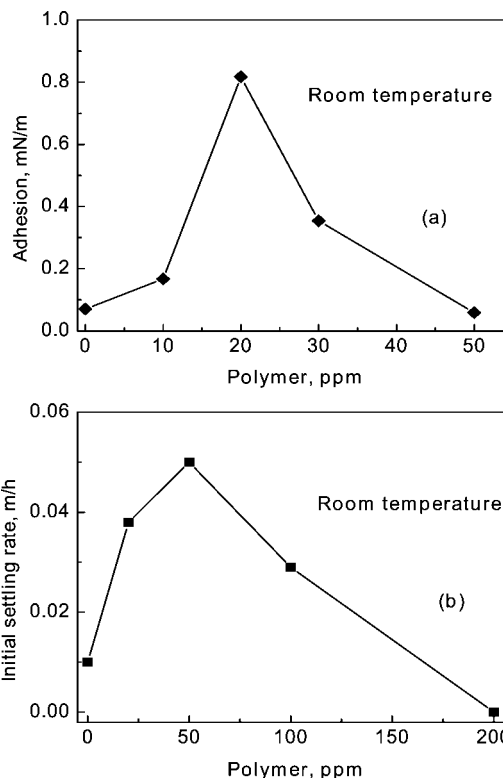


**Figure 10. (a) Average adhesion forces as a function of polymer dosage at room temperature; (b) initial settling rate as a function of polymer dosage.**

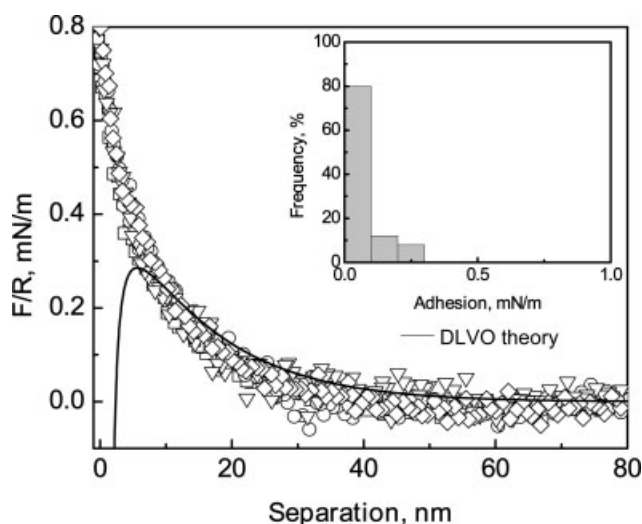


**Figure 11. Long-range interaction and adhesion forces between kaolinite particles in a 1 mM KCl solution in the absence of poly(NIPAM) at pH  $\approx$  8.6 and 40°C.**

The solid curve is the DLVO force profile using  $\kappa^{-1} = 12.67$  nm,  $A = 2.20 \times 10^{-20}$  J and a fitted potential of  $-50$  mV. The inset shows the adhesion force distribution.

In this case, both kaolinite surfaces were possibly fully covered by the adsorbed polymers and the adsorbed polymers set a steric barrier to prevent kaolinite particles from approaching each other. The absence of adhesion indicates that the kaolinite particles hardly attached to each other. Such a condition would indicate a stable kaolinite suspension. This was verified by our settling tests where the addition of 200 ppm polymer into the suspension caused the initial settling rate to be almost zero, indicating that the suspension was very stable.

Figure 10 shows the average adhesion force and the initial settling rate as a function of poly(NIPAM) dosage at room temperature. Both the average adhesion force (Figure 10a) and initial settling rate (Figure 10b) as a function of poly(NIPAM) dosage exhibit a similar trend. The average adhesion and the initial settling rate first increased with increasing polymer dosage to an optimal dosage, followed by a decrease with further increasing the dosage, although the maximum was achieved at different dosages. This finding indicates a clear correlation between the adhesion force and the initial settling rate: the higher the adhesion force, the higher the initial settling rate. The difference in polymer dosages where the maximum is located is attributed to the different surface areas of kaolinite clay particles in the two test systems. The suspension contained a large number of kaolinite particles, whereas there were only a few kaolinite particles in the AFM force measurement. As a result, the surface area of kaolinite particles in the suspension is much larger than that in the AFM experiments, thereby decreasing the polymer concentration in the water. It is evident that further polymer addition is required in settling tests than in AFM force measurement to ensure a similar availability of polymer molecules to kaolinite particles in both systems. This translates to a lesser amount of polymers needed in AFM force measurement to achieve the maximum adhesion force.

**Results Obtained at 40°C.** As mentioned earlier, poly(NIPAM) exhibited a better flocculation behavior using proce-

cedure B than procedure A. To understand this difference in the settling experiments, the long-range interaction and adhesion force measurements between kaolinite particles were conducted following a temperature-changing procedure similar to that used in procedure B, that is, the solution was first injected into the fluid cell at room temperature, then the solution was heated to and maintained at 40°C during the force measurement. Figure 11 shows the long-range interaction and adhesion forces between kaolinite particles in a 1 mM KCl solution at pH 8.6. Compared with the long-range repulsive forces at room temperature (Figure 6), the long-range repulsion at 40°C was stronger. The classical DLVO theory was used to fit the measured long-range force profiles. In the fitting procedure, the Hamaker constant ( $A$ ) was the same as that used to calculate DLVO forces at room temperature (Figure 6). The decay length ( $\kappa^{-1}$ ) as a function of temperature was calculated to be 12.67 nm at 40°C using the following equation:<sup>31</sup>

$$\kappa^{-1} = \left\{ \frac{\epsilon \epsilon_0 k_B T}{e^2 \sum n_i(\infty) z_i^2} \right\}^{1/2}$$

where  $e$  is the charge on electron,  $n_i(\infty)$  is the number per unit volume of the electrolyte ions of type  $i$  with valence  $z_i$  in the bulk solution far from the surface,  $k_B$  is Boltzmann's constant,  $T$  is the absolute temperature in Kelvin,  $\epsilon_0$  is the permittivity of vacuum, and  $\epsilon$  is the relative permittivity of the solution. The zeta potential value of kaolinite clay particles ( $\psi$ ) was set as an adjustable parameter. Figure 11 shows that by using a zeta potential value of  $-50$  mV, the long-range repulsive forces were in substantial accord with the classical DLVO theory, suggesting that the surface potential of kaolinite particles became more negatively charged (from  $-35$  to  $-50$  mV) when the temperature increased from room temperature to 40°C. Ramachandran and Somasundaran<sup>36</sup> also found that the surface of kaolinite particles became more negatively charged with

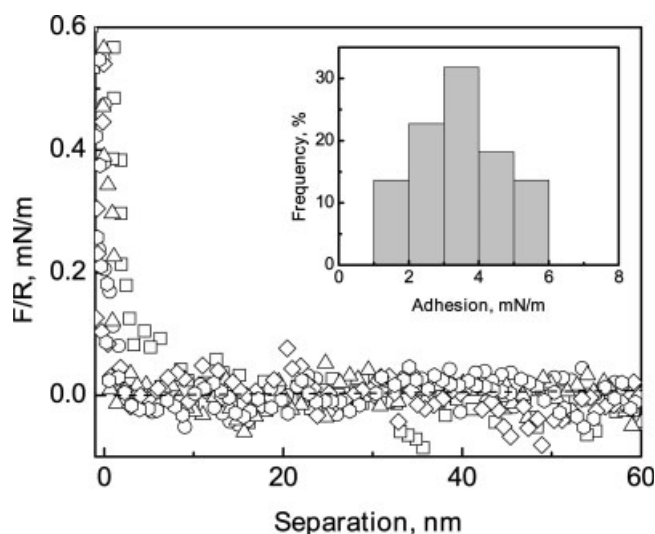


**Figure 12. Long-range interaction and adhesion forces between kaolinite particles in a 1 mM KCl solution at pH  $\approx$  8.6 in the presence of 50 ppm poly(NIPAM) at 40°C.**

The inset shows the adhesion force distribution.



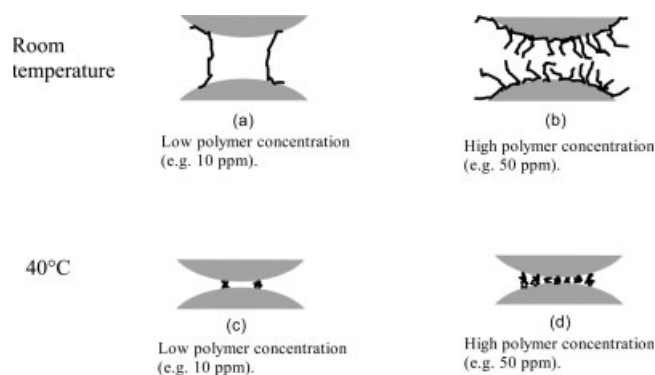


**Figure 13. At room temperature.**

(a) Low polymer concentration (e.g., 10 ppm). The surface of the particles was partially covered by the adsorbed polymer molecules with a stretched structure. Bridging was formed between the two particles by the adsorbed polymers. (b) High polymer concentration (such as 50 ppm). The surface of the particles was fully covered by the adsorbed polymer molecules. A steric repulsion was caused by the extruded polymer tails. At 40°C: (c) Low polymer concentration (such as 10 ppm). Bridging was formed between two particles by the adsorbed polymers with a coil-like structure. (d) High polymer concentration (such as 50 ppm). The surface coverage of the particles by the adsorbed polymers was increased. More polymer bridges were formed between the two particles by the adsorbed polymer molecules.

increasing temperature. For the kaolinite surface, an increase in temperature would favor the formation of  $\text{Al}(\text{OH})_4^-$  and  $\text{H}_3\text{SiO}_4^-$  groups, thus resulting in a more negative charge. The adhesion force as shown in the inset of Figure 11 was nearly zero. Based on the long-range and adhesion forces, the kaolinite suspension is anticipated to be stable in a 1 mM KCl solution at pH 8.6. As discussed earlier, without polymer addition using procedure B, the initial settling rates was 0.03 m/h, indicating a stable suspension and supporting the implications from the AFM force measurements.

Figure 12 shows the long-range interaction and adhesion forces between kaolinite particles in a 1 mM KCl solution containing 50 ppm poly(NIPAM) at pH 8.6 and 40°C. Compared with the results obtained without polymer addition (Figure 11), 50 ppm poly(NIPAM) addition suppressed the long-range repulsive force to nearly zero. The adhesion force increased drastically to 3.5 mN/m. The weak long-range repulsion and strong adhesion forces between kaolinite particles indicate that the kaolinite suspension in the presence of 50 ppm polymer will be flocculated quickly. This expectation was verified by our settling results using procedure B. As shown in Figure 5, in the presence of 500 ppm poly(NIPAM), the initial settling rate increased to 2.0 m/h and the sediment volume after a settling period of 120 min decreased to 28 mL.

Comparison of the AFM results at room temperature with those at 40°C at the same polymer dosage of 50 ppm (Figures 9 and 12) indicates much weaker long-range repulsive forces and much stronger adhesion forces when the measurement was performed at 40°C. This observation confirms that the good flocculation of a kaolinite suspension at a higher polymer dosage using procedure B is attributed to the substantially weak repulsive long-range forces and stronger adhesion forces between the kaolinite particles. The difference in the adhesion force obtained at 40°C and that at room temperature can be

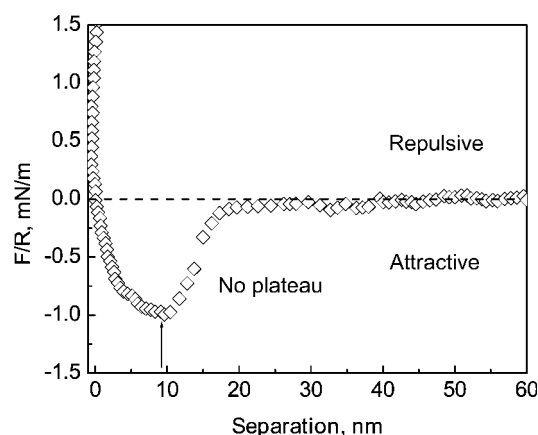


**Figure 14. A typical retraction force profile obtained between kaolinite particles in a 1 mM KCl solution in the presence of 20 ppm poly(NIPAM) at pH  $\approx$  8.6 and 40°C.**

attributed to the difference in binding strengths of polymer with clay particles and polymer conformation.

Figure 13 illustrates the effect of poly(NIPAM) concentration on the interaction between two particles at room temperature and 40°C, respectively. At room temperature, the polymer molecule has a stretched structure. At a low polymer concentration (such as 10 ppm), the particle surfaces were only partially covered by the adsorbed polymers (Figure 13a). Some free surface areas were still available for polymer adsorption. Under such a condition, the dangling tails/loops of the polymer molecules on one surface could contact and be adsorbed onto the other surface, exhibiting bridging adhesion. With increasing polymer concentration, the surface coverage of the particles by the polymers was increased. The number of the formed polymer bridges was increased, resulting in an increased adhesion force (such as 0.8 mN/m at a polymer concentration of 20 ppm). At a high polymer concentration (say 50 ppm), the particle surface was fully covered by the adsorbed polymers (Figure 13b). A steric barrier was set by the extruded tails of the adsorbed polymers, thereby preventing the two particles from approaching each other, leading to a strong long-range repulsion and a negligible adhesion. At 40°C, poly(NIPAM) molecules became coiled. At a low polymer concen-

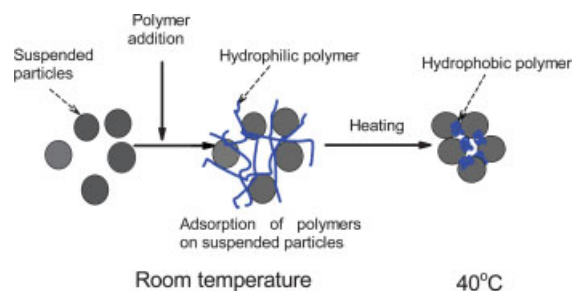


**Figure 15. A schematic diagram of the flocculation mechanism using a temperature-sensitive polymer [poly(NIPAM)] under procedure B.**

[Color figure can be viewed in the online issue, which is available at [www.interscience.wiley.com](http://www.interscience.wiley.com).]



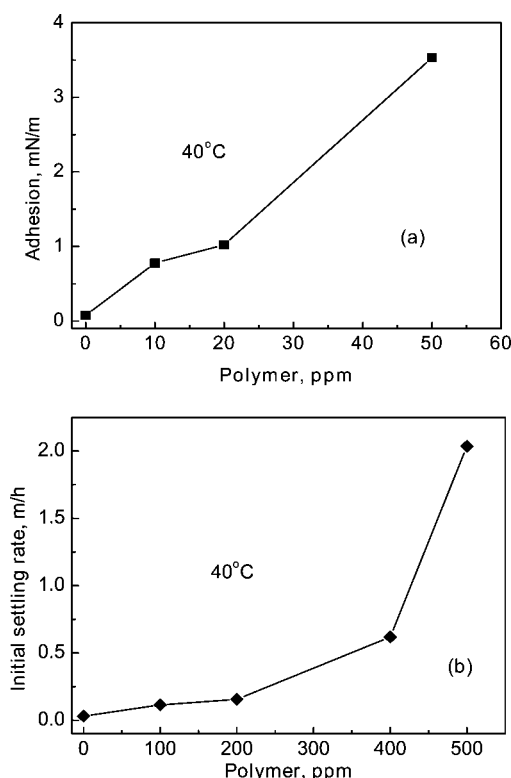


**Figure 16. (a) Average adhesion forces as a function of polymer dosage at 40°C; (b) initial settling rate as a function of the polymer dosage using settling procedure B.**

tration (such as 10 ppm), the adsorbed polymers caused a partial coverage of the particle surface (Figure 13c). Bridging was formed between the two particles by the adsorbed polymers with a coil-like structure. At a high polymer concentration (such as 50 ppm), the surface coverage of the particles by the adsorbed polymers increases. Because the polymer molecule was coiled, the surface of the particles was still partially covered (Figure 13d). The number of polymer bridges was significantly increased, resulting in a strong adhesion force (such as 3.5 mN/m at a polymer concentration of 50 ppm).

The coil-like conformation of the polymer molecule was verified by the AFM results. Figure 14 shows a typical retraction force profile in the presence of 20 ppm poly(NIPAM) at 40°C. A detachment at a separation distance of 9 nm was observed, indicating a very compacted structure of the adsorbed polymer on the kaolinite surface, whereas the retraction profile obtained at room temperature (Figure 8a) shows a plateau of about 60 nm, that is, a long stretch of polymer molecules, indicating an extended structure. These results and interpretation are consistent with other studies.<sup>37,38</sup>

The conformational change of poly(NIPAM) molecule is related to its chemical structure. As shown in Figure 1b, there is a hydrophilic group ( $-\text{CONH}-$ ) and a hydrophobic group [ $-\text{CH}(\text{CH}_3)_2$ ] on the polymer side chain. Ramon et al.<sup>39</sup> and Katsumoto et al.<sup>40</sup> found that in an aqueous solution relatively strong hydrogen bonds were formed between the hydrophilic group ( $-\text{CONH}-$ ) and water molecules at room temperature. Thus, the polymer became soluble and exhibited an extendable

structure. When the temperature was increased, hydrogen bonds between the hydrophilic groups and water molecules were broken and intramolecular hydrogen bonds,  $\text{C}=\text{OH}-\text{N}$ , were formed. As a result of such intramolecular interactions, the polymer molecules became coiled.

Figure 15 shows a schematic diagram of the flocculation mechanism using poly(NIPAM) under procedure B. The polymer molecules with a stretched structure were first mixed with a clay suspension at room temperature. Under such a condition, particles could adsorb onto different sites of the long extended polymer chains. When the temperature was increased to 40°C, the polymer chain became coiled. The adsorbed particles were then brought together, leading to compacted flocs and thus inducing a faster settling.

Figure 16 shows the average adhesion force and the initial settling rate as a function of poly(NIPAM) dosage at 40°C. The trends of the average adhesion forces (Figure 16a) and the initial settling rate in response to the change of poly(NIPAM) dosage (Figure 16b) are similar; that is, they both increased with increasing polymer dosage.

## Conclusions

In this study, a temperature-sensitive polymer [poly(NIPAM)] was synthesized and used as a flocculant to treat kaolinite clay suspensions. Two settling procedures were used. In procedure A, both mixing and settling were carried out at room temperature. In procedure B, mixing was carried out at room temperature, but settling was conducted at a higher temperature of 40°C. The following conclusions can be drawn from this study.

(1) Suspension temperature shows an important impact on the settling rate. Poly(NIPAM) exhibits a better flocculation performance with a wider operational dosage range using procedure B than using procedure A.

(2) Results of AFM force measurement were consistent with the settling results. A weaker long-range repulsive force and a stronger adhesion force were obtained at 40°C.

(3) Poly(NIPAM) molecules exhibit a long, extended structure at room temperature and a coil-like conformation at a higher temperature (40°C). It is this conformational change of the polymer molecules that results in a better settling using procedure B than that using procedure A.

## Acknowledgments

Financial support from NSERC Industrial Research Chair in Oil Sands Engineering (held by JHM) is gratefully acknowledged.

## Literature Cited

- Chalaturnyk RJ, Scott JD, Özüim B. Management of oil sands tailings. *Petrol Sci Technol*. 2002;20:1025–1046.
- Matthews JG, Shaw WH, MacKinnon MD, Cuddy RG. Development of composite tailings technology at syncrude. *Int J Surf Mining Reclam Environ*. 2002;16:24–39.
- Hamza HA, Stanonik DJ, Kessick MA. Flocculation of lime-treated oil sands tailings. *Fuel*. 1996;75:280–284.
- Cymerman G, Kwong T, Lord E, Hamza H, Xu Y. Polymers in mineral processing. Proceedings of the 3rd UBC-McGill Biannual International Symposium on Fundamentals of Mineral Processing. Quebec City, QC, Canada, Aug. 22–26;1999:605–619.

5. Xu Y, Cymerman G. Polymers in mineral processing. Proceedings of the 3rd UBC-McGill Biannual International Symposium on Fundamentals of Mineral Processing. Quebec City, QC, Canada, Aug. 22–26; 1999:591–604.
6. Igarashi C, Sakohara S. *Separation of Solid and Liquid in Suspensions Using Ionic Temperature-sensitive Polymer Flocculants*. Japanese Patent No. 2001-232104; 2001.
7. Heskins M, Guillet JE. Solution properties of poly(N-isopropylacrylamide). *J Macromol Sci Chem A2*. 1968;1441–1451.
8. Schild HG. Poly(N-isopropylacrylamide): Experiment, theory and application. *Prog Polym Sci*. 1992;17:163–249.
9. Ito S. Phase transition of aqueous solution of poly(N-alkylacrylamide) derivatives: Effects of side chain structure. *Kobunshi Ronbunshu*. 1989;46:437–443.
10. Guillet JE, Heskins M, Murray DG. *Polymeric Flocculants*. U.S. Patent No. 4536294; 1985.
11. Sakohara S, Kimura T, Nishikawa K. Flocculation mechanism of suspended particles utilizing hydrophilic/hydrophobic transition of thermo-sensitive polymer. *Kagaku Kogaku Ronbunshu*. 2000;26:734–737.
12. Sakohara S, Nishikawa K. Flocculation and compaction of highly concentrated suspension using thermo-sensitive polymers. *Kagaku Kogaku Ronbunshu*. 2000;26:298–304.
13. Igarashi C, Sakohara S. Solid-liquid separation method for suspension using heat sensitive polymer flocculant. Japanese Patent No. 2000-237506, 2000.
14. Atago Y, Maruyama T, Kido O, Oka H. Temperature-sensitive Flocculating Agents. Japanese Patent No. 4298203; 1992.
15. Bremmell KE, Jameson GJ, Biggs S. Polyelectrolyte adsorption at the solid/liquid interface. Interaction forces and stability. *Colloids Surf A: Physicochem Eng Aspects*. 1998;139:199–211.
16. Abraham T, Kumpulainen A, Xu Z, Rutland M, Claesson PM, Masliyah JH. Polyelectrolyte-mediated interaction between similarly charged surfaces: Role of divalent counter ions in tuning surface forces. *Langmuir*. 2001;17:8321–8327.
17. Vigil G, Xu Z, Steinberg S, Israelachvili J. Interaction of silica surfaces. *J Colloid Interface Sci*. 1994;165:367–385.
18. Kamiyama Y, Israelachvili J. Effect of pH and salt on the adsorption and interactions of an amphoteric polyelectrolyte. *Macromolecules*. 1992;25:5081–5088.
19. Long J, Xu Z, Masliyah JH. Role of illite-illite interactions in oil sands processing. *Colloids and Surfaces A*. 2006;281:202–214.
20. Diplas P, Papanicolaou AN. Batch analysis of slurries in zone settling regime. *J Environ Eng*. 1997;123:659–667.
21. Li H, Long J, Xu Z, Masliyah JH. Synergetic role of polymer flocculant in low-temperature bitumen extraction and tailings treatment. *Energy Fuels*. 2005;19:936–943.
22. Liu JF, Min G, Ducker WA. AFM study of adsorption of cationic surfactants and cationic polyelectrolytes at the silica–water interface. *Langmuir*. 2001;17:4895–4903.
23. Liu J, Xu Z, Masliyah JH. Studies on bitumen–silica interaction in aqueous solutions by atomic force microscopy. *Langmuir*. 2003;19:3911–3920.
24. Ducker WA, Senden TJ, Pashley RM. Measurement of forces in liquids using a force microscope. *Langmuir*. 1992;8:1831–1836.
25. Robinovich YI, Yoon RH. Use of atomic force microscope for the measurements of hydrophobic forces between silanated silica plate and glass sphere. *Langmuir*. 1994;10:1903–1909.
26. Liu J, Xu Z, Masliyah JH. Role of fine clays in bitumen extraction from oil sands. *AIChE J*. 2004;50:1917–1927.
27. Barbara HS. *Polymer Analysis*. New York: Wiley; 2002:106–108.
28. Fujishige S. Intrinsic viscosity–molecular weight relationships for poly(N-isopropylacrylamide) solutions. *Polym J*. 1987;19:297–300.
29. Mpofu P, Addai-Mensah J, Ralston J. Temperature influence of non-ionic polyethylene oxide and anionic polyacrylamide flocculation and dewatering behavior of kaolinite dispersions. *J Colloid Interface Sci*. 2004;27:145–156.
30. Mpofu P, Addai-Mensah J, Ralston J. Investigation of the effect of polymer structure type on flocculation, rheology and dewatering behaviour of kaolinite dispersions. *Int J Miner Process*. 2003;71:247–268.
31. Israelachvili JN. *Intermolecular and Surface Forces*. 2nd Edition. San Diego, CA: Academic Press; 1992.
32. Hunter JR. *Introduction to Modern Colloid Science*. New York: Oxford Univ. Press; 1993.
33. Warszynski P, Adamczyk Z. Calculations of double-layer electrostatic interactions for the sphere/plane geometry. *J Colloid Interface Sci*. 1997;187:283–295.
34. Liu J, Zhou Z, Xu Z, Masliyah JH. Bitumen–clay interactions in aqueous media studied by zeta potential distribution measurement. *J Colloid Interface Sci*. 2002;252:409–418.
35. Liu J. Role of colloidal interaction in bitumen recovery from oil sands. *Ph.D. Thesis*. University of Alberta, Edmonton, Canada; 2004.
36. Ramachandran R, Somasundaran P. Effect of temperature on the interfacial properties of silicates. *Colloids Surf*. 1986;21:355–369.
37. Zareie HM, Volga Bulmus E, Gunning AP, Hoffman AS, Piskin E, Morris VJ. Investigation of a stimuli-responsive copolymer by atomic force microscopy. *Polymer*. 2000;41:6723–6727.
38. Kanazawa H. Temperature-responsive polymers for liquid-phase separations. *Anal Bioanal Chem*. 2004;378:46–48.
39. Ramon O, Kesselman E, Berkovici R, Cohen Y, Paz Y. Attenuated total reflectance/Fourier transform infrared studies on the phase-separation process of aqueous solutions of poly(N-isopropylacrylamide). *J Polym Sci Part B: Polym Phys*. 2001;39:1665–1677.
40. Katsumoto Y, Tanaka T, Ozaki Y. Relationship between the coil-globule transition of an aqueous poly(N-isopropylacrylamide) solution and structural changes in local conformations of the polymer. *Macromol Symp*. 2004;205:209–223.

Manuscript received July 5, 2006, and revision received Oct. 28, 2006.